reactions

MDPI

Article

Valorization of Microcrystalline Cellulose Using Heterogeneous Protonated Zeolite Catalyst: An Experimental and Kinetics Approach

Samuel Kassaye [1], Dinesh Gupta [1], Kamal Kishore Pant [1] and Sapna Jain [2,*]

[1] Department of Chemical Engineering, Indian Institute of Technology Delhi, Hauz Khas, New Delhi 110016, India; samiselam@gmail.com (S.K.); dineshguptakp@gmail.com (D.G.); kkpant@chemical.iitd.ac.in (K.K.P.)
[2] Department of Physical and Forensic Sciences, Alabama State University, Montgomery, AL 36104, USA
* Correspondence: sjain@alasu.edu; Tel.: +1-334-604-9320

Abstract: This study aimed to valorize microcrystalline cellulose (MCC) using protonated zeolite catalysts such as (H-ZSM-5) and Cr/H-ZSM-5 (5%) in ionic liquid. The catalytic effect in synergy with 1-butyl-3-methylimidazolium Chloride ([BMIM] Cl) ionic liquid was studied in detail. The total reducing sugar (TRS) was determined using the 3, 5-dinitrisalcylic acid (DNS) array method. The catalysts were characterized using techniques such as Fourier transform infrared (FT-IR), X-ray diffraction analysis (XRD), temperature-programmed desorption of ammonia (NH_3-TPD), and BET-surface area analyzer. H-ZSM-5 effectively depolymerized cellulose with a maximum yield of 70% total reducing sugar (34% glucose, 8% fructose, and 4.5% 5-HMF). Cr/H-ZSM-5 catalyst dehydrated fructose to 5-HMF with a yield of 53%. The use of ionic liquid significantly reduced the activation energy of formation and decomposition. The activation energy determined in cellulose hydrolysis was 85.83 KJ mol^{-1} for a reaction time of 180 min while the decomposition energy was found to be 42.5 kJ mol^{-1}.

Keywords: microcrystalline cellulose; ionic liquid; hydrolysis; kinetic modeling

Citation: Kassaye, S.; Gupta, D.; Pant, K.K.; Jain, S. Valorization of Microcrystalline Cellulose Using Heterogeneous Protonated Zeolite Catalyst: An Experimental and Kinetics Approach. *Reactions* **2022**, *3*, 283–299. https://doi.org/10.3390/reactions3020021

Academic Editors: Wenping Ma and Ajay K. Dalai

Received: 24 March 2022
Accepted: 19 May 2022
Published: 30 May 2022

1. Introduction

Efficient and economic conversion of lignocellulosic biomass (LCB) to value-added chemicals in integrated biorefinery is believed to reduce the dependency on a nonrenewable resource such as fossil fuel. LCB is a promising feedstock for the biorefinery industry to produce biofuel and valuable chemicals from renewable sources [1]. Successful utilization of biomass demands the effective conversion of the cellulosic portion of LCB to develop integrated biorefinery to produce biofuel and chemicals economically. The hydrolysis of cellulose strongly depends on its properties, such as degree of polymerization and crystallinity. The utilization of lignocellulosic biomass depends on the level of success achieved in hydrolysis of the cellulose into its monomeric form, glucose [2]. However, cellulose is the most recalcitrant and well-known crystalline biopolymer due to its extensive intra- and inter-hydrogen bonding network. Cellulose is a structurally linear polymer composed of glucose monomers joined together by β-1, 4-glycosidic linkage [3]. Therefore, it is difficult to dissolve and subsequently hydrolyze cellulose using conventional organic solvents including water and ethanol [4,5].

The hydrolysis of cellulosic biomass is carried out using an enzymatic approach accompanied by a high glucose yield at moderate reaction conditions. Enzymatic hydrolysis has several disadvantages related to the high cost of enzymes, limited cellulose conversion, and scalability challenges [3]. Hydrolysis of cellulose using acidic catalysts such as liquid acids including mineral and organic acids is another alternative option [6]. Mineral acids are highly efficient in breaking β-1, 4-glucosidic linkage [7,8]. However, this method

has several drawbacks: reaction product decomposition, difficulty in the product, and catalyst separation. Mineral acid catalysts are also known to cause reactor corrosion, costly post-treatment, challenges in recycling catalysts and consumption of a large amount of neutralizing agents [9,10]. As a result, attempts are underway to apply solid acid catalysts to convert lignocellulosic biomass to biochemicals. The application of ionic liquids further improves this approach. Some selected ionic liquids have inherent characteristics allowing them to dissolve cellulose and disrupt the hydrogen bonding network effectively.

Ionic liquids (ILs) are low-melting-point organic salts that can be utilized both as solvents and catalysts to convert lignocellulosic biomass [11]. The suitability of ILs for biomass utilization is attributed mainly to their tunable physico-chemical properties, such as viscosity, polarity, and thermal stability. ILs act as non-volatile polar solvents and can dissolve the complex cellulosic materials. The use of ILs allows production flexibility with high efficiency while eliminating the use of undesirable volatile solvents. In this regard, solid acid catalysts such as zeolites, ion exchange resins, and zirconia are considered an alternative chemo-catalytic approach for cellulose depolymerization. Zeolite-based solid acid catalysts have tremendous advantages compared to homogeneous catalysts, such as easy separation, recyclability, and adjustable surface acidity [12].

Zeolite catalysts have been modified and used in industrial processes as milestones in history and have brought about profound changes in the petrochemicals industry. For example, zeolite Y's use in the Fluid Catalytic Cracking (FCC) process significantly increased fuel production efficiency. HZSM-5, which has an 8- to 10-member ring with a pore size between 0.5 and 56 nm, is well-suited for bio-refinery. However, cellulose insolubility in aqueous media has been the greatest hurdle to applying zeolites as solid acid catalysts due to solid–solid formation, which limits mass transfer and reactivity. However, ionic liquids with unique properties allowing them to dissolve cellulose and reduce its crystallinity are able to convert cellulose to value-added chemicals [13,14].

ZSM-5 has also been widely used as a catalyst for biomass pyrolysis, for it has excellent deoxidation properties that reduce the oxygenated compounds and increase aromatic compounds during the bio-oil production. This is especially helpful as the bio-oil containing a higher aromatic species content can be profitably upgraded to gasoline and diesel fuel. H^+-exchanged ZSM-5 (H-ZSM-5) removes oxygen from the biomass due to its strong dehydration tendency promoted by its strong acidic nature. Strong acidity of H-ZSM-5 may result in over-cracking of hydrocarbon and result in a decrease in organic components in bio-oil; therefore, there is a need to fine-tune the acidic sites required for catalytic action. Studies have revealed that transition-metal-impregnated ZSM-5 catalysts(Ni-ZSM-5, Fe-ZSM-5, Ce-ZSM-5) have been found to be more effective in increasing acidic sites, resulting in a higher hydrocarbon yield and less coke production than the commercial ZSM-5 catalyst [15–18].

Zeolites inherently possess both Bronsted and Lowry as well as Lewis acid sites. These acidic sites help catalyze and promote hydrolysis of cellulose, isomerization of glucose, and fructose dehydration [19]. The H-ZSM-5 catalyst was the choice of this study due to its inherent properties, such as strong and active acid sites suitable for a catalyst with a porous structure and larger surface area. These properties enhance and facilitate the depolymerization of cellulose to produce bio-chemicals. In this research work, the catalytic effects of H-ZSM-5 and Cr/H-ZSM-5 (5%) were studied to depolymerize MCC. The experimental results show that the synergy between ionic liquid and H-ZSM-5 improved cellulose conversion and the yield of the desired bio-chemicals.

2. Materials and Methods

2.1. Materials

All the chemicals used were of analytical grade (purity 99.9%). Extra-pure microcrystalline cellulose with an average particle size of 90μm was purchased from Alfa Aesar (A Johnson Matthey Company, Heysham, Lancashire, United Kingdom). As reported in our previous research work [20], the original MCC's initial crystallinity index was found to

be 76%, which reduced to 42% due to the influence of the ionic liquid. 1-Chlorobutane, N-methyl imidazole, toluene, acetone acetonitrile, ethyl acetate, 3, 5-dinitrisalcylic acid, sodium hydroxide, sodium potassium tartrate phenol, acetonitrile, cellulose, and isopropanol were purchased from Fisher Scientific (Anand Bhuvan, Princess Street Mumbai, India). H-ZSM-5 with Si/Al ratio of 30 was obtained from Sud-chemie India. [BMIM] Cl ionic liquid was prepared and characterized as reported in our previous work [20].

2.2. Methods

2.2.1. Catalyst Synthesis and Characterization

Chromium-impregnated H-ZSM-5 (Cr/H-ZSM-5) catalyst was prepared using wet impregnation method in which H-ZSM-5 was mixed with chromium precursor ($CrCl_3 \cdot 6H_2O$) in 50 mL of distilled water [21]. The mixture was stirred vigorously for 3 h at 80 °C, and then the excess solvent was removed by rotary evaporator at reduced pressure. Subsequently, the sample was dried overnight at 120 °C and calcined at 500 °C for 5 h. The catalysts were characterized using Fourier transform infrared spectroscopy (FTIR, Thermo scientific NICOLET iS50 attenuated total reflectance-Fourier transform spectroscopy (ATR-FTIR)), X-ray powder diffractometer (XRD, Rigaku miniflex 600, Tokyo, Japan), Brunauer–Emmett–Teller (BET, ASAP 2010 Micromeritics, Santa Rosa, CA, USA) surface area, temperature-programmed desorption of ammonia (TPD, Micromeritics Pulse Chemisorb 2720, Norcross, GA, USA), and thermo-gravimetric analysis (TGA, TGA-Q600 instrument, New Castle, DE, USA). The thermal properties of both catalysts were studied using thermo-gravimetric analysis (TGA). The analysis was performed using nitrogen gas as a purge gas at a flow rate of 30 mL per min with a heating rate of 20 °C per min from 30 to 1000 °C.

Temperature-programmed desorption of ammonia (NH_3-TPD) was performed to determine the total acid strength and acid site distribution on the surface of both catalysts using the Micromeritics Pulse Chemisorb 2720 instrument. The chemisorb instrument is equipped with a quartz reactor and a thermal conductivity detector (T.C.D). The sample catalyst (0.2 g) was pretreated at 250 °C for 2 h with a continuous flow of pure helium gas to remove the moisture content at room temperature. The sample was then saturated with 10% ammonia gas for adsorption for 1 h. After complete saturation, physiosorbed ammonia was removed by flowing helium for 30 min. The TPD was carried out in a stream of helium gas, raising the temperature from 50 °C to 980 °C at the rate of 10 °C per min. The desorption process of ammonia was monitored using a T.C.D detector, and the amount of total desorbed ammonia was obtained from the integrated peak area of the TPD profiles relative to the calibration curve.

2.2.2. Catalytic Hydrolysis

The hydrolysis of MCC was performed using a batch reactor 250 mL in size where the dissolution of MCC was performed in [BMIM] Cl ionic liquid with 1:20 w/w proportion. The stirring was carried out continuously for 30 min until the mixture turned homogeneous. Then, 5 mL of distilled water and H-ZSM-5 (1:2 w/w ratio of MCC to H-ZSM-5) was added, and the solvent was returned to the reactor using a condenser. On the completion of the reaction time, the reaction mixture was quenched using an ice bath. Then, the catalyst and the hydrolysate were separated using vacuum filtration process. The hydrolysate was centrifuged at 10,000 rpm for 10 min and then stored in a refrigerator for further analysis.

2.2.3. Hydrolysis Product Analysis

The samples were analyzed using dinitrosalicyclic acid (DNS) reagent in UV-Vis spectroscopy for TRS yield while HPLC was used to determine the yield of sugars and dehydration products. DNS analysis hydrolysate was mixed with DNS reagent in 1:2 v/v ratio and boiled for 10 min in a water bath. The resulting solution was cooled using an ice bath, and the analysis was carried out by measuring the absorbance of the sample using UV–Vis spectroscopy (CARY 100Conc) at 540 nm wavelength. The total reducing sugar

yield was determined from the calibration curve formed using four-point concentration of standard glucose solutions. The yield of TRS was calculated using Equation (1).

Fructose, glucose, and 5-HMF were analyzed using high-performance liquid chromatography (HPLC). The HPLC analysis was performed using Agilent technology 1200 infinity equipped with Bio-Rad Aminex HPx-87H 300 × 7.8 mm columns, UV detector for sugar dehydration product, and RI detector for sugar products. The eluent was 5 mM sulfuric acid with a flow rate of 0.6 mL per minute, and the injection volume was 20 µL. The identification of products in the sample was performed using a pure form of the products to determine retention time and calibration curve formation. The 5-HMF was calculated as given below in Equation (2).

3. Result and Discussion

3.1. Catalyst Characterization

The catalyst was characterized using Fourier transform infrared (FT-IR), X-ray diffraction analysis (XRD), BET (Brunauer–Emmett–Teller) surface area, temperature-programmed desorption of ammonia (ammonia TPD), and the thermo-gravimetric analysis method (TGA analysis) as discussed below.

3.1.1. FT-IR Analysis

FT-IR is generally used to characterize the structure of adsorbed species by analyzing the bonds absorbed in the functional group region ranging from 4000 to 1500 cm^{-1}. It can also be used to deduce reaction mechanisms and acidic properties by distinguishing the bond type and construction mode between various functional groups or atoms. Interactions between a transition-metal atom and a hydrocarbon activates the hydrocarbon, which is responsible for the conversion of hydrocarbons into value-added chemicals [22]. The incorporation of chromium metal into the zeolite can play a significant role in alteration of the catalyst structure as well as the product yield. The interactions weaken the C–H and C–C bonds of a hydrocarbon and therefore facilitate the rearrangement of the bonds and atoms into more valuable platform chemicals [23]. In order to construct efficient and promising homogeneous and heterogeneous catalysts, an understanding of the activation process of the C–H and C–C bonds in hydrocarbons is important. The Dewar–Chatt–Duncanson model explains the coordinative binding of the transition-metal atom to the unsaturated hydrocarbon [24]. The π and π^* orbitals of alkenes and alkynes match the d orbitals of the transition metals, which result in electron transfer from the chromium cation to the π^* orbital of unsaturated hydrocarbons, C_2H_2 or C_2H_4, due to the orbital interactions. In this study, we also revealed that confinement of chromium cations within the ZSM-5 cavities exhibits unique catalytic behavior [25]. The results of FTIR analysis are supported by XRD analysis, and the shift in the peak of Cr/H-ZSM-5 catalyst is attributed to the increase in interplanar d-spacing due to chromium metal's presence in the zeolite framework.

H-ZSM-5 and Cr/H-ZSM-5 catalysts were characterized by the FTIR method to study the effect of chromium metal incorporation in the framework structure of the H-ZSM-5 catalyst. The FTIR spectra of H-ZSM-5 and Cr/H-ZSM-5 catalysts range between 500 and 2000 cm^{-1}, as shown in Figure 1. The result shows that sensitive structural bands of H-ZSM-5 and Cr/H-ZSM-5 catalysts have similar positions. This implies that chromium metal incorporation in the zeolite structure was too insignificant to alter the basic zeolite structure and functional groups. The absorption bands at 1225, 1088, 810, and 540 cm^{-1} are considered as the characteristic signals for the framework vibration of the H-ZSM-5 zeolite catalyst. It was found that the band 540 cm^{-1} belongs to the T–O (T=Si or Al) vibration of the internal tetrahedral, 540 cm^{-1} to the double ring, 810 cm^{-1} to the external symmetric stretch, 1088 cm^{-1} to the internal asymmetric stretch, and 1225 cm^{-1} to the external asymmetric stretch, respectively [26,27]. The internal vibrations of SiO_4 and AlO_4 are represented by the absorption bands at 1088 and 810 cm^{-1}, respectively [28]. The perturbation of bands at around 920–905 cm^{-1} could be due to the internal asymmetric

T-O-T by Cr 920–905 cm^{-1}, Cr-O-Si. Similarly, the bands near 540 and 1225 cm^{-1} are assigned to the double-ring vibration and asymmetric stretching.

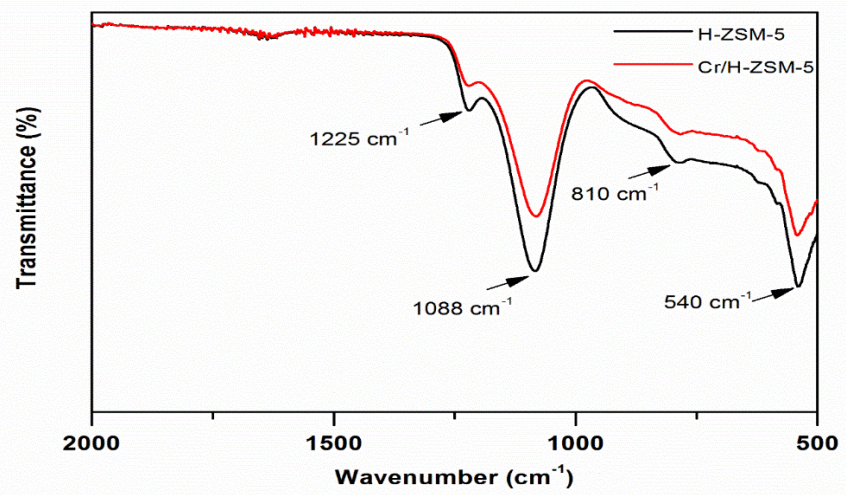

Figure 1. FTIR analysis of H-ZSM-5 and Cr/H-ZSM-5 catalysts.

3.1.2. XRD Analysis

Figure 2 shows the XRD spectra pattern of H-ZSM-5 and Cr\H-ZSM-5. The XRD data analysis was used to study the effect of chromium metal incorporation on the framework structure of the H-ZSM-5 catalyst. The intensity and the number of diffraction peaks of both catalysts were similar, and there is no indication of significant change in the XRD pattern. However, the peak of the Cr/H-ZSM-5 catalyst showed a slight shift to the left. According to the Bragg equation, this shift in the peak of Cr/H-ZSM-5 catalyst is attributed to the increase in interplanar d-spacing due to chromium metal's presence in the framework [29]. This observation is supported by FTIR analysis where the perturbation of bands at around 920–905 cm^{-1} could be due to the internal asymmetric T-O-T by Cr 920–905 cm^{-1}, Cr-O-Si. This indicates that the bigger lattice parameters represent the inclusion of atoms of different diameters. However, extra diffraction peaks were not observed, representing uniform dispersion of chromium throughout the zeolite framework structure [30].

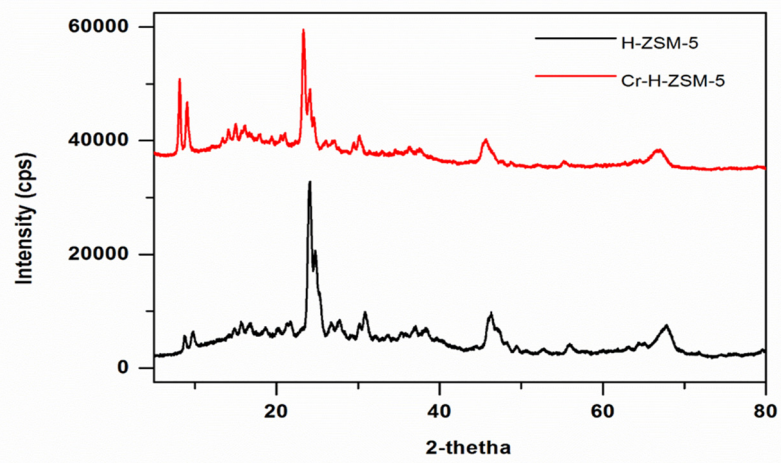

Figure 2. XRD pattern of H-ZSM-5 and Cr/H-ZSM-5 catalysts.

3.1.3. BET Analysis

The introduction of transition metal into zeolite often causes the changes in the textural properties, such as porosity, pore type, micropore surface area, and micropore volume of zeolite [31]. BET surface area analysis is frequently used to determine the surface area,

pore size, and pore volume of a catalyst to make an estimation of the catalytic activity of a catalyst. The catalysts with greater porosity usually show greater activity because of an increased surface area [32].

The BET surface area analysis for H-ZSM-5 and Cr/H-ZSM-5 is given in Table 1. According to the results, the surface area of H-ZSM-5 decreased after the impregnation of chromium metal. Impregnation of chromium metal into H-ZSM-5 led to a decrease in surface area from 270 to 248 m^2 g^{-1} due to the partial pores blocking H-ZSM-5 structural support by chromium metal [33].

Table 1. BET surface area analysis of H-ZSM-5 and Cr/H-ZSM-5 catalysts.

Catalyst Type	BET Surface Area (m^2/g)
H-ZSM-5	270.0
Cr/H-ZSM-5	248.2

3.1.4. Ammonia-TPD Analysis

NH_3-TPD analysis is usually used to characterize the number of acidic sites, acid strength, and types of acid sites in zeolites [34]. The amount of ammonia desorbed at a given temperature range is directly proportional to the acid site [35]. Generally, the peaks observed in the temperature range of 100–200 °C correspond to the weak acid center. The peaks in the temperature range of 350–400 °C are due to the moderately strong acid center, whereas the high-temperature peaks between 400 and 600 °C correspond to the strong acid center. Thus, the medium and strong acid sites can be designated as Brønsted acid sites, and weak acid sites can be designated as Lewis acid sites, and they also indicate a weak adsorption of NH_3 [36].

The acid site property of the catalysts was studied using temperature-programmed desorption of ammonia (Ammonia-TPD). As presented in Figure 3, the catalysts' acid site distribution was determined using the desorption peaks. The result shows the effect of chromium metal impregnation into the framework structure on the acidity of H-ZSM-5. The entire surface acid sites of Cr/H-ZSM-5 qualitatively increased compared to H-ZSM-5, implying the presence of additional acid sites due to the inclusion of chromium into the H-ZSM-5 structure [37]. For H-ZSM-5, the low-temperature peak was observed at a temperature between 150 and 300 °C, while the high-temperature peak was observed between 300 and 500 °C, representing the low and high desorption peaks, respectively.

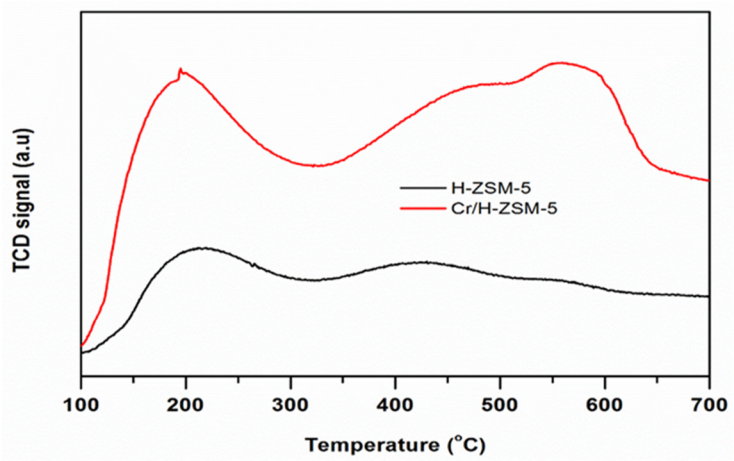

Figure 3. Ammonia-TPD analysis of H-ZSM-5 and Cr/H-ZSM-5 catalysts.

The framework of the zeolite used in this study had a Si/Al ratio of 30, which may have affected the incorporation of chromium into zeolite crystals, which, finally, affected the chromium content, the size and distribution of chromium species, acid sites, surface area,

interaction of metal carriers, thermal stability, and catalytic performance of the Cr-H-ZSM-5 catalyst [38]. It is known that the dispersion of metal depends on the number of ion sites available within the zeolite framework [37]. The lower the Si/Al ratio, the higher the number of ionic sites, the better the dispersion, and the greater the amount of chromium on the ionic sites. Even though chromium impregnation reduced the surface area, as revealed by BET surface area analysis, NH_3-TPD studies revealed a significant increase in the acid site and hence explain the enhanced catalytic activity of the Cr-H-ZSM-5 catalyst.

Similarly, the Cr/H-ZSM-5 catalyst showed the acid site distribution at a low temperature of 200–300 °C while the high-temperature peak formed at 350–650 °C. The peak at low and high temperature indicates the presence of weak and strong acid sites, respectively. In general, the incorporation of chromium metal into the frameworks of H-ZSM-5 increased both the strong and the weak acid sites. However, the effect on strong acid sites was more significant than on the weak acid sites, which is consistent with the literature [32].

3.2. Hydrolysis of MCC

In a preliminary study, hydrolysis of MCC was performed in the absence of the H-ZSM-5 catalyst, [BMIM] Cl, and prior to dissolution as a reference. Compared with the reference, the hydrolysis reaction was significantly influenced by the prior dissolution in ionic liquid and the catalytic amount of H-ZSM-5. In this condition, 70% maximum yield of TRS was achieved at a temperature of 180 °C, reaction time of 180 min, and catalyst-to-substrate loading ratio of 2:1 (w/w). The high sugar yield from the prior dissolution process is attributed to the structural change from microcrystalline to amorphous cellulose due to the ionic liquid effect [5]. The ionic liquid used was potent enough to break the hydrogen bonding networks which hold the cellulose strand together. As a result, cellulose's crystallinity reduced significantly, facilitating the accessibility of cellulose to the acid sites of the H-ZSM-5 catalyst. The exposure of the acid sites broke the glycosidic bonds of the glucose monomers. In similar experimental work under identical conditions except for the absence of a catalyst, hydrolysis reaction yielded 6% of TRS, which is exceptionally low, signifying the catalyst's effective yield. In addition, hydrolysis without prior dissolution resulted in 8% TRS yield. In this case, the low yield of TRS was due to solid–solid interactions of the cellulose substrate and H-ZSM-5. Prior dissolution of cellulose decreased the crystallinity and degree of polymerization, which improved the H-ZSM-5 catalyst and the substrate's interaction. In this condition, the dissolved MCC easily migrated to the catalyst's active surface to cause the breakdown of the glycosidic bonds to release the sugar monomers. The higher conversion of cellulose and maximum yield of TRS were obtained due to improved interaction of the MCC substrate with the catalyst.

Figure 4 shows the hydrolysis of MCC and the effect of temperature on the yield of hydrolysis products. The effectiveness of the hydrolysis of MCC in the catalytic effect of H-ZSM-5 in the presence of [BMIM] Cl ionic liquid was studied based on TRS, glucose, fructose, and 5-HMF yield. The hydrolysis reaction results at the different temperatures indicate that the maximum yield of TRS was obtained at 180 °C, whereas for glucose, the maximum yield was obtained at 190 °C. The TRS yield showed an increase as the temperature was raised from 160 °C to 180 °C. However, the yield showed a decreasing trend as temperature further increased due to the decomposition of TRS. As seen in Figure 4, the hydrolysis of MCC was significantly affected by reaction temperature and time. The results imply a maximum of 70% TRS comprising 34% glucose, 8% fructose, and 4.5% 5-HMF at a temperature of 180 °C and hydrolysis time of 180 min. Similarly, the effect of hydrolysis time on the yield of TRS, glucose, and fructose at different temperatures showed that the product yield was significantly affected by reaction time. The yield of TRS increased with time and reached a maximum of 180 min of hydrolysis time. Afterward, the TRS yield decreased due to the decomposition of sugars because of the extended reaction time. As can be observed from Figure 2, the depolymerization of cellulose using the H-ZSM-5 catalyst in [BMIM] Cl ionic liquid resulted in an increasing trend and decreased when the depolymerization time was extended. Cellulose hydrolysis carried out for a run time

of 180 min and at a catalyst-to-substrate ratio of 2:1 resulted in a sharp increase in TRS yield as the temperature increased from 160 °C (44% yield of TRS) to 180 °C (70% yield of TRS). However, further raising the temperature from 180 °C to 200 °C deceased the yield to 60%. This was due to the decomposition of sugars such as glucose and fructose as the temperature was increased above 180 °C for 180 min of hydrolysis time.

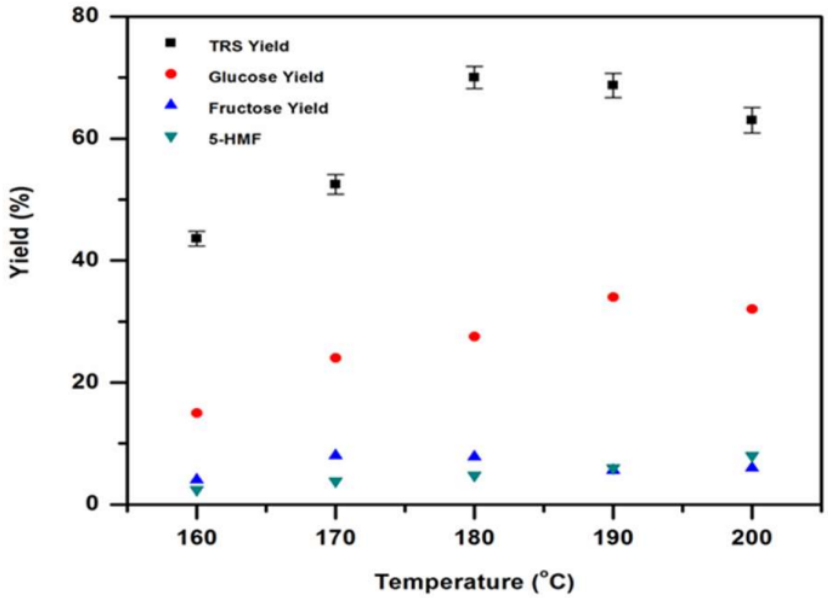

Figure 4. Effect of hydrolysis temperature on TRS yield (catalyst-to-substrate ratio of 2:1 (*w*/*w*) and 180 min of reaction time).

For a comparative study, the experiments were carried out in a round-bottom flask kept in an oil bath. The experimental process was as follows: 0.1 g cellulose was dissolved in 2.0 g of [BMIM] Cl at a predetermined dissolution temperature and time, and then a catalytic amount of H-ZSM-5 catalyst and 5 mL of distilled water were added to the mixture. The depolymerization of MCC was carried out via two main steps: first through the prior dissolution of MCC in [BMIM] Cl ionic liquid followed by hydrolysis by solid acid catalysts, H-ZSM-5 and Cr/H-ZSM-5. The purpose of prior dissolution with [BMIM] Cl ionic liquid was to break the structural network of hydrogen bonding in cellulose to achieve easier interaction between the catalyst and substrate. Preliminary experimental results were compared between the two catalysts for effective depolymerization of MCC for further investigation. It was found that the H-ZSM-5 catalyst showed better catalytic activity and was able to depolymerize MCC with a maximum yield of 70% total reducing sugar, while the Cr/H-ZSM-5 catalyst yielded a maximum of 55%. However, Cr/H-ZSM-5 achieved a higher yield of 5-HMF from fructose (53%) while H-ZSM-5 obtained a maximum yield of 31% with identical reaction conditions. The weak catalytic ability of the of Cr/H-ZSM-5 to depolymerize MCC to total reducing sugar was due to a reduction in Bronsted acid sites due to chromium metal inclusion, which generally increases the Lewis acidity at the expense of Bronsted acid sites. For cellulose hydrolysis, higher Bronsted acidity is required to cleave the glycosidic bond, while for sugar dehydration, both acidities' optimized acid sites play an essential role.

In transforming lignocellulosic biomass to value-added chemicals such as 5-HMF and LA, fructose is considered the ideal substrate with a more straightforward conversion and excellent yield of 5-HMF, using a wide range of homogeneous as well as heterogeneous catalysts. For instance, chromium chloride ($CrCl_2$, $CrCl_3$) and copper chloride catalysts in an ionic liquid have been reported to be effective for dehydration of sugars to form 5-HMF with a maximum yield of 81% from fructose and 70% using glucose [39,40]. However, the challenge in separation and the high level of chromium toxicity hinders the practical

production of 5-HMF. Heterogeneous acid catalysts are easily recovered and have high production sustainability, making them more promising for practical applications in large-scale production than homogenous catalysts [41]. Therefore, catalytic dehydration of fructose to 5-HMF using chromium metal impregnated on H-ZSM-5 support (5% Cr/H-ZSM-5) was tested and resulted in 87% conversion and 55% yield of 5-HMF in [BMIM] Cl-water reaction media. In this study with identical reaction conditions, the yield of 5-HMF using the Cr/H-ZSM-5 catalyst was found to be effective compared with the yield obtained from the H-ZSM-5 catalyst (H-ZSM-5). Therefore, further investigation was carried out to study the effect of temperature and dehydration time on 5-HMF yield.

The effect of temperature and reaction time on the dehydration of fructose catalyzed by Cr/H-ZSM-5, using [BMIM] Cl-water as a solvent, was studied. The yield of 5-HMF showed a pattern of increasing and then decreasing with time at all temperatures studied as shown in Figure 5. At 160 °C, the yield of 5-HMF increased gradually to 34% over 60 min, while at 180 °C, it increased rapidly to 53% after 30 min, showing that a higher temperature increased the yield of 5-HMF and decreased the dehydration time required. This was further confirmed at 200 °C with a of yield 47% 5-HMF at 15 min of dehydration time. The maximum yield was achieved at a temperature of 180 °C and 30 min of reaction time. When the dehydration reaction time was extended over 30 min, the yield of 5-HMF decreased significantly due to decomposition of 5-HMF. The degradation products contained levuilinic acid, formic acid, and soluble polymers, as observed in HPLC analysis. However, the separated products were far too small to be quantified. In the case of soluble polymers, a wide range of products are possibly available, making it very difficult to obtain the accurate molecular structure and determine the exact product type [41].

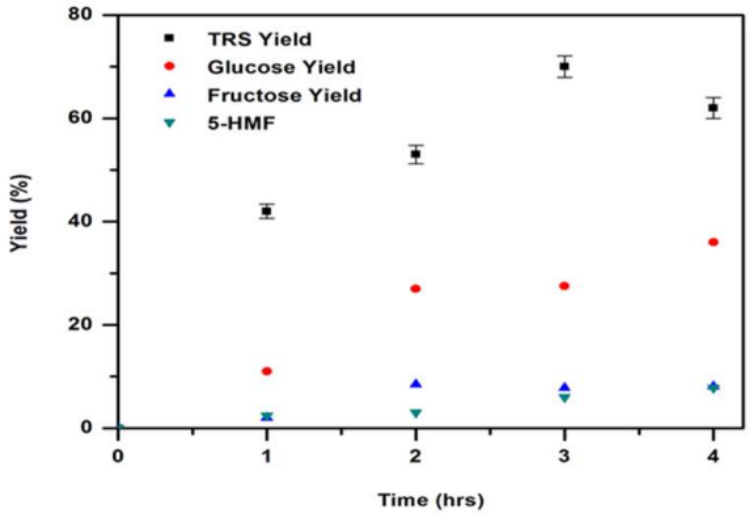

Figure 5. Effect of hydrolysis time on the yield of TRS (temperature 180 °C, catalyst-to-substrate ratio of 2:1 (*w*/*w*)).

The reaction temperature and time had a significant influence on the conversion of glucose to 5-HMF. The conversion of glucose to 5-HMF at a temperature of 200 °C and 60 min of reaction time yielding a maximum yield of 24% 5-HMF was achieved. The results suggest that as temperature increased, the yield of 5-HMF also increased initially and then followed a decreasing pattern over the extended reaction time due to the formation of undesired products such as insoluble humin and soluble polymers [42]. Moreover, the formation of 5-HMF from glucose at 160 °C and 180 °C after 120 min of reaction time resulted in maximum yields of 17 and 19.5% HMF, respectively. The dehydration of glucose is relatively complex compared with fructose due to the six-membered pyranoside structure. For this reason, the dehydration of glucose to 5-HMF requires an additional step of isomerization of glucose to fructose before the dehydration reaction to form 5-HMF using the Cr/H-ZSM-5 catalyst.

3.2.1. Mechanism of MCC Hydrolysis

During the hydrolysis of MCC, two steps are essential: the dissolution of MCC in [BMIM] Cl ionic liquid and the subsequent hydrolysis in the presence of water as a cosolvent using a catalytic amount of the H-ZSM-5 catalyst. The purpose of dissolution of MCC alone in the ionic liquid is primarily to overcome cellulose's recalcitrant behavior and break the hydrogen bonding networking in the cellulose strand. This step is essential to improve the accessibility of β-1, 4-glycosidic linkages between the glucose and create contact between the substrate and catalyst within the reaction media. Besides, prior dissolution helps simplify the structural complexity of cellulose, resulting in higher crystallinity and a more significant degree of cellulose polymerization to ease hydrolysis. Mechanistically, the chlorine ions of the ionic liquid are efficient in forming a new hydrogen bond with the hydroxyl groups of cellulose while the cations prevent the crosslinking of cellulose in the dissolution process. The cations form a linkage with the oxygen of the broken hydroxyl groups of the cellulose and serve as electron acceptors (Figure 6).

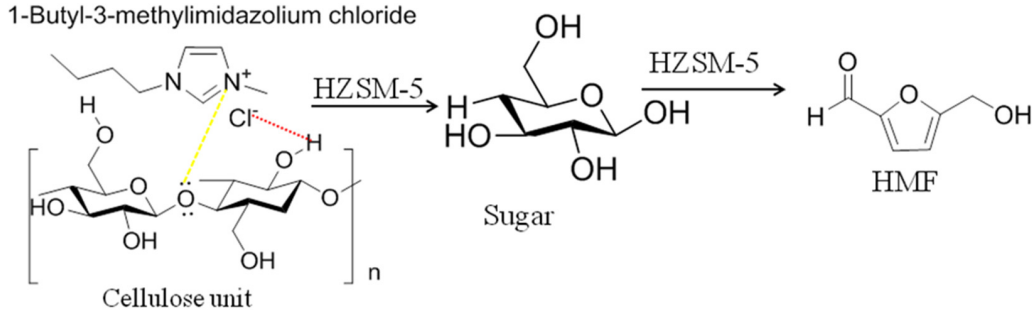

Figure 6. Mechanism of cellulose hydrolysis with H-ZSM-5 catalyst in the presence of [BMIM] Cl ionic liquid.

The hydrolysis of MCC, as described by the Saeman model [43], involves the reaction kinetics following two pseudo-homogeneous consecutive first-order reactions. The degradation products are mainly 5-HMF and humins. The mechanism of MCC hydrolysis with the H-ZSM-5 catalyst is like the hydrolysis of cellulose in the presence of homogeneous acidic catalysts such as sulfuric acids. The glycosidic bonds in the cellulose polymer are broken by Bronsted acid sites similar to H^+ ions of acidic solutions to release the glucose monomers through binding with the glycosidic oxygen atom, leading to hydrolysis of MCC to simple sugars. H^+ cations generated in situ from the Bronsted acid sites of zeolite are the key active species for the effective hydrolysis of cellulose with H-ZSM-5, and the Lewis acid sites do not exhibit high activity as reported by FT-IR through pyridine adsorption [19]. In addition to the catalyst, the H^+ molecules produced from the dissociation of water (co-solvent) participate in the hydrolysis reaction, facilitating the glycosidic bond's cleavage.

3.2.2. Kinetic Modeling of MCC Depolymerization

Valorization of lignocellulosic biomass requires understanding the mechanism and kinetics of the complex cellulose hydrolysis reaction [44]. The complexity of cellulose hydrolysis emerges from the recalcitrant behavior of cellulose, which requires harsh reaction conditions. The hydrolysis products (sugars) have high reactivity that suffers from further decomposition under severe reaction conditions. The incompatibility between the cellulose stability and highly reactive hydrolysis products complicates understanding the reaction mechanism and kinetics of cellulose hydrolysis. However, understanding the mechanism and kinetics of the hydrolysis reaction is especially important for process design and optimization. The kinetic modeling for cellulose hydrolysis in the synergetic effect of the H-ZSM-5 catalyst and [BMIM] Cl ionic liquid has been studied to investigate the ionic liquid's effect on the rate of reaction, activation energy, and mechanism of hydrolysis.

The yield data of TRS were obtained experimentally, and data were generated from the mathematical model (Equation (4)). The activation energy and reaction rate constants (k_1 and k_2) were calculated and compared, and the results are presented in Figure 3. The experiments were performed over a wide temperature range (140 to 200 °C) and hydrolysis run time (0 to 180 min). The kinetic model used is a model developed by Saeman for cellulose hydrolysis, and the present study assumed irreversible pseudo-homogeneous first-order reactions [45]. The estimation of the kinetic parameters was performed using Polymath 6.0 software. The following assumptions were taken into consideration for model development:

1. The first step in depolymerization of microcrystalline cellulose is the cleavage of β-(1, 4) glycosidic bonds followed by decomposition of TRS to other products, namely 5-HMF and humin.
2. The reaction rate equations were developed based on the Saeman model considering all the model's assumptions [46]. Primarily, the model assumes irreversible pseudo-homogeneous first-order reactions.
3. The TRS concentration was based on MCC's hydrolysis reaction, which includes the major depolymerization products intermediate sugars and oligomers.
4. Mass transfer on the reaction kinetics was insignificant due to the complete dissolution of cellulose in [BMIM] Cl ionic liquid media before the depolymerization reaction.
5. It was assumed that dissolved cellulose diffuses into the internal pores of zeolite and the glycosidic bonds of cellulose and then extends into the vicinity of Bronsted acid sites where catalytic depolymerization takes place [46].

Hydrolysis of lignocellulosic biomass is an overly complex reaction comprising formation and decomposition of sugars. Therefore, a simplified kinetic model was used to describe the formation and decomposition of sugar products from cellulose's hydrolysis. The model proposes that cellulose depolymerization involves the hydrolysis of cellulose to reducing sugar and subsequent degradation of sugar to furan chemicals and humin. The reaction scheme for depolymerization of cellulose is shown in Equation (1), while the reaction rate constant for the second-series reaction, i.e., TRS decomposition, is given in Equation (2).

$$\text{Cellulose} \xrightarrow{K_1} \text{TRS (Glucose)} \xrightarrow{K_2} \text{TRS Decomposition products} \quad (1)$$

$$\text{A} \xrightarrow{K_1} \text{TRS B} \xrightarrow{K_2} \text{TRS C} \quad (2)$$

The formation rate of reducing sugars (B) with respect to depolymerization time is represented by Equation (4). The integration of Equation (4) (considering the following boundary conditions at t = 0, $C_{B,0} = 0$) with respect to time gives Equation (6), which was used to represent the concentration of total reducing sugar production as a function of time and used to calculate the reaction constants (k_1 (min^{-1}) and k_2 (min^{-1})). The Arrhenius equation describes the correlation of reaction rate constants with the temperature. The activation energies were calculated from the Arrhenius equations with a reference temperature. The batch reaction rate of formation of the reactions is given as follows:

$$-r_A = k_1 C_A \quad (3)$$

$$r_B = k_1 C_A - k_2 C_B \quad (4)$$

$$r_C = k_1 C_A \quad (5)$$

The concentration of TRS with time can be calculated as shown in Equation (6) below:

$$C_B = k_1 C_{AO} \left(\frac{e^{-k_1 t} - e^{-k_2 t}}{k_2 - k_1} \right) \quad (6)$$

where C_A is the cellulose concentration (mg mL^{-1}), C_{A0} is the initial concentration of cellulose (mg mL^{-1}), C_B is the total reducing sugars concentration (mg mL^{-1}), CC is decomposition product concentration, and 't' is the depolymerization reaction time (min).

3.2.3. Formation and Degradation of TRS

The application of ionic liquid for catalytic hydrolysis of cellulose to value-added chemicals is a promising approach to overcome the recalcitrant nature of cellulose for a potential scale-up to the bio-refinery scheme. The presence of [BMIM] Cl ionic liquid improved the yield of interest products from microcrystalline cellulose's depolymerization. The role of [BMIM] Cl was significant for three reasons: (1) [BMIM] Cl dissolved cellulose entirely within the given substrate loading, (2) the chloride ions in the ionic liquid played the role of base and nucleophile, which promoted the isomerization of glucose to fructose, and (3) [BMIM]+ of the ionic liquid stabilized dehydration products and prevented further decomposition [47]. The dissolution temperature and time showed a profound effect on reducing the crystallinity index and degree of cellulose polymerization. The higher the crystallinity and degree of polymerization of cellulose, the lower the reactivity to depolymerize to sugar monomers. Therefore, it is imperative to dissolve cellulose and reduce its crystallinity to hydrolyze the substrate effectively. The reduction in crystallinity was achieved through the prior dissolution of cellulose in an ionic liquid followed by the hydrolysis reaction using the catalytic effect of the H-ZSM-5 catalyst.

A kinetic model was constructed based on calculating the best-fit reaction coefficients for k_1 and k_2, as presented in Table 2. The model fitted well with the experimental data for all four temperature sets with an R^2 value greater than 0.96, showing reasonable agreement between the experimental and calculated data. Figure 7 shows the kinetic data compared with the experimental result. It can be observed that the activation energies of formation and decomposition of sugars decreased significantly for [BMIM] Cl ionic liquid media compared with the hydrolysis that takes place in aqueous media [31]. The activation energy of cellulose's depolymerization to reducing sugars (Ea1 = 85.8 kJ mol^{-1}) was less than the calculated activation energy for acid hydrolysis of cellulose in water (Ea1 = 105–188 kJ mol^{-1}) [9]. The activation energy values reported for cellulose hydrolysis using an ionic liquid solvent fell in the range from 55 to 89 kJ mol^{-1}, depending on the nature of the ionic liquid and the cosolvent effect [10].

Table 2. Kinetic rate constants at different temperatures.

Temperature (°C)	k_1 (min^{-1})	k_2 (min^{-1})
140	0.0010	0.0006
160	0.0042	0.0019
180	0.0094	0.0020
200	0.0244	0.0035

Similarly, the activation energy for decomposition of reducing sugars in ionic liquid was lower (Ea2 = 42.5 kJ mol^{-1}) than that for aqueous media (Ea2 = 120 kJ mol^{-1}). The decrease in activation energies for the consecutive reactions can be attributed to the ionic liquid's ionic nature, enhancing the susceptibility of glycosidic bond cleavage to release the sugar monomers. The plot of ln (k) vs. 1/T leads to a straight line with a slope of the fitting line indicating the activation energy, and the pre-exponential factor is determined by the intercept of the fitting curve, as shown in Figure 8 and reported in the literature, [32] for both formation and decomposition of reducing sugar from the depolymerization of cellulose.

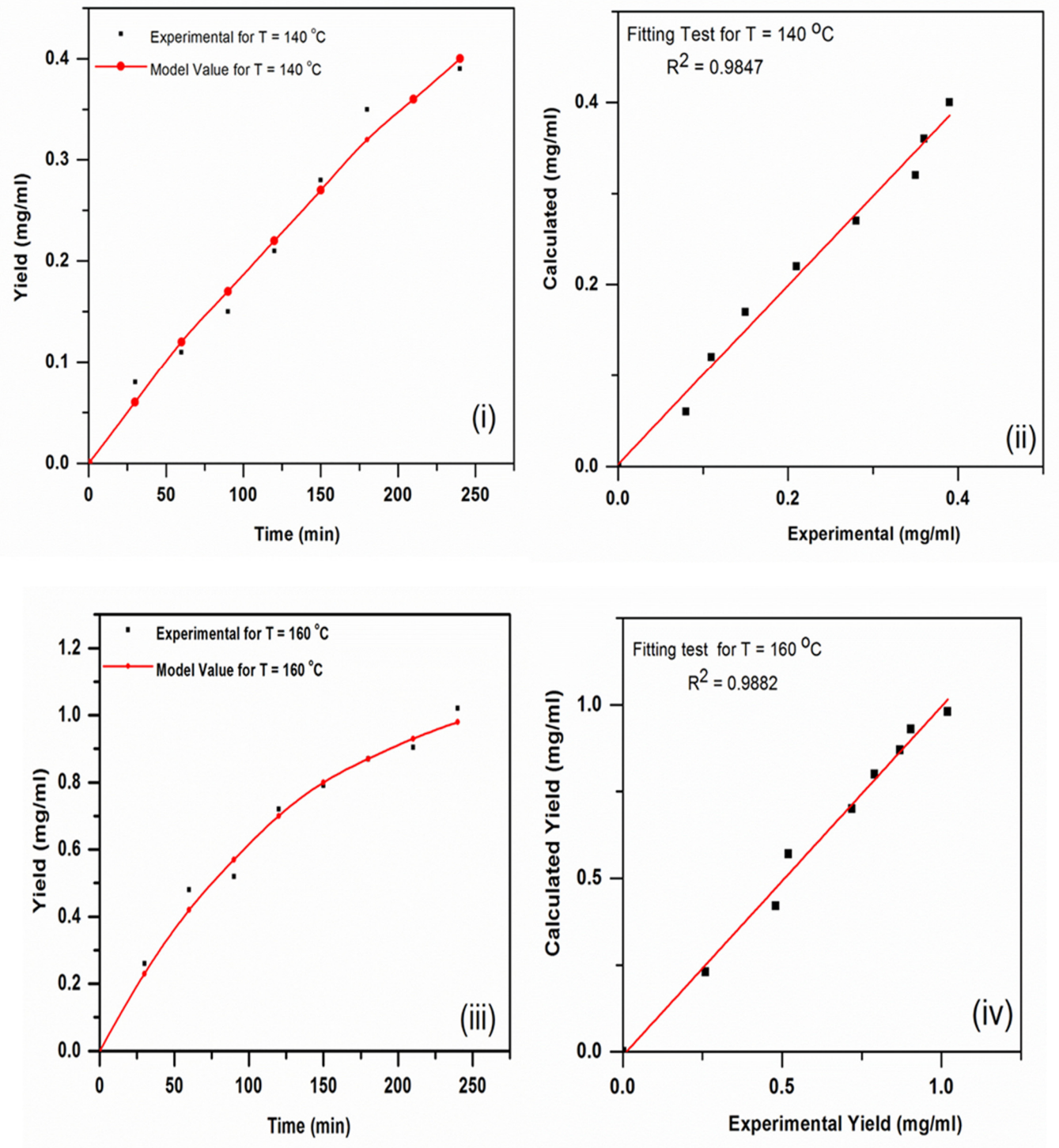

Figure 7. *Cont.*

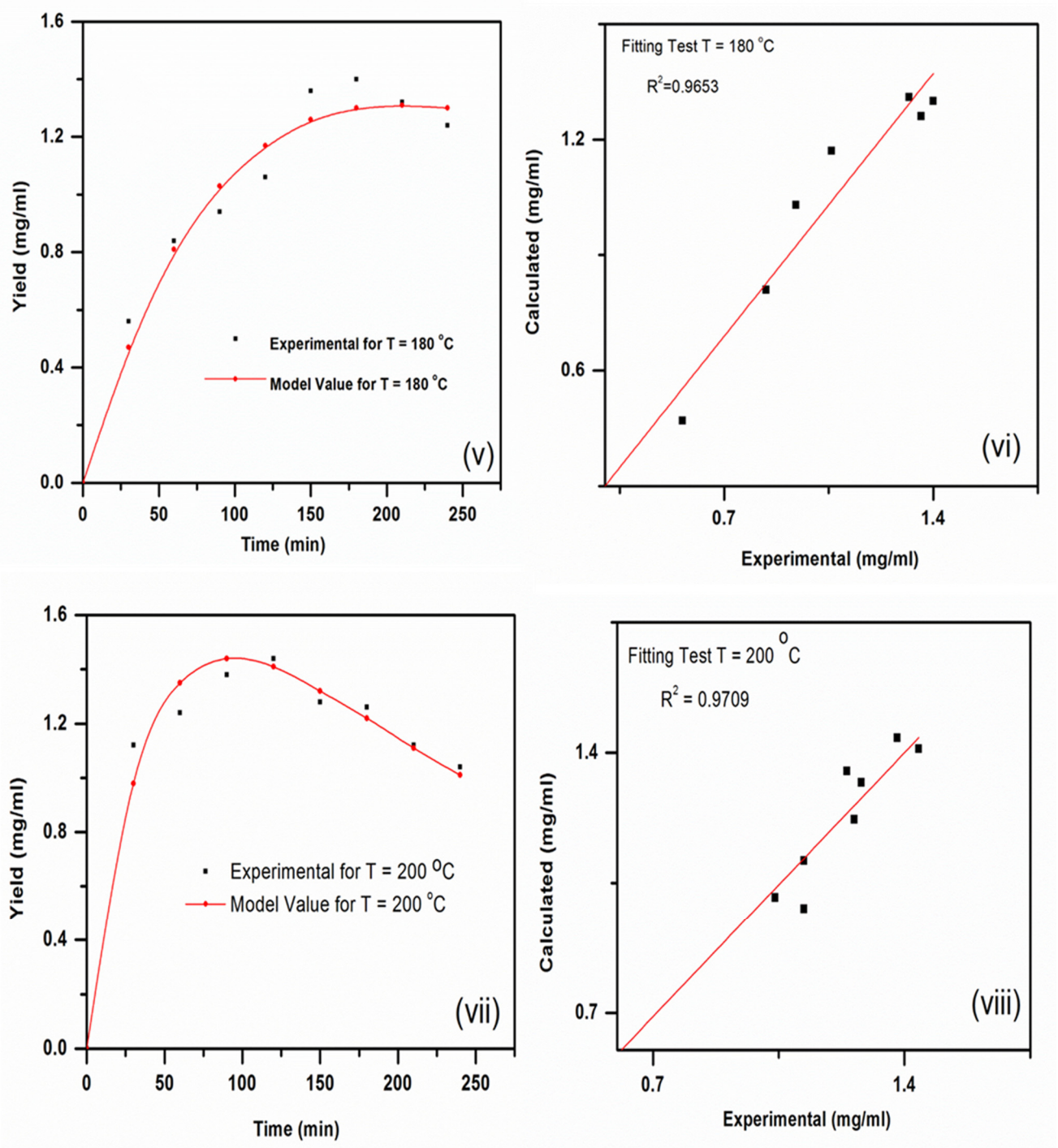

Figure 7. Kinetic modeling of cellulose hydrolysis using H-ZSM-5 catalyst in [BMIM] Cl-water media. (**i**) Experimental and model data at 140 °C, (**ii**) Fitting test at 140 °C, (**iii**) Experimental and model data at 160 °C, (**iv**) Fitting test at 140 °C, (**v**) Experimental and model data at 180 °C, (**vi**) Fitting test at 180 °C, (**vii**) Experimental and model data at 200 °C, (**viii**) Fitting test at 200 °C.

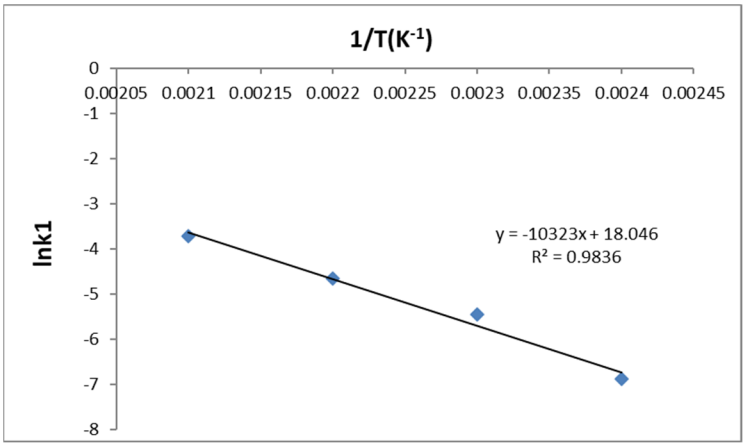

(a)

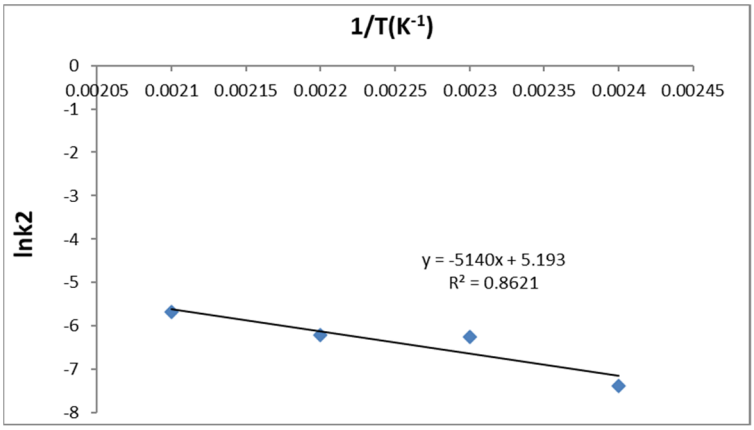

(b)

Figure 8. Determination of rate constants for cellulose hydrolysis using H-ZSM-5 catalyst in [BMIM] Cl. (**a**) plot of ln (k) vs. 1/T for K_1, (**b**) plot of ln (k) vs. 1/T for K_2.

4. Conclusions

The inert nature of cellulose and insufficient knowledge of solid–solid reaction systems make the heterogeneous catalytic conversion of cellulose ambitious. In our research, porous zeolite materials (H-ZSM-5) and ionic liquid showed an extraordinary ability to perform as catalysts and catalyst support for cellulose conversion. It appears that the mechanism of action of the zeolite catalyst involves the breaking of the glycosidic bonds in cellulose to release the glucose monomers. The closeness of the acidic sites may be essential for cellulose hydrolysis as acidic strength alone may not be sufficient.

A kinetic study of MCC hydrolysis using the synergistic effect of [BMIM] Cl ionic liquid was performed with H-ZSM-5. The catalyst was adequate for the MCC's depolymerization up to a yield value of 70% TRS. [BMIM] Cl ionic liquid was highly influential in overcoming cellulosic biomass's recalcitrance by breaking the extensive network of intra- and inter-hydrogen bonding, and the strong acidity of H-ZSM-5 was able to break the beta-1, 4-glycosidic bond to release sugar molecules. During the depolymerization reaction, ionic liquid's presence significantly reduced the activation energy of both the formation and decomposition of sugar obtained from the reaction. The activation energy calculated for cellulose hydrolysis using H-ZSM-5 for a depolymerization time of 180 min was found to be 85.8 kJ mol^{-1}, while the decomposition of reducing sugars in ionic liquid was found to be 42.5 kJ mol^{-1}.

Author Contributions: Investigation, S.K., S.J.; Formal analysis, D.G.; Supervision, K.K.P. All authors have read and agreed to the published version of the manuscript.

Funding: This research received no external funding.

Conflicts of Interest: The authors declare no conflict of interest.

References

1. Chimentão, R.J.; Lorente, E.; Gispert-Guirado, F.; Medina, F.; López, F. Hydrolysis of dilute acid-pretreated cellulose under mild hydrothermal conditions. *Carbohydr. Polym.* **2014**, *111*, 116–124. [CrossRef] [PubMed]
2. Ji, W.; Shen, Z.; Wen, Y. Hydrolysis of wheat straw by dilute sulfuric acid in a continuous mode. *Chem. Eng. J.* **2015**, *260*, 20–27. [CrossRef]
3. Auxenfans, T.; Buchoux, S.; Djellab, K.; Avondo, C.; Husson, E.; Sarazin, C. Mild pretreatment and enzymatic saccharification of cellulose with recycled ionic liquids towards one-batch process. *Carbohydr. Polym.* **2012**, *90*, 805–813. [CrossRef] [PubMed]
4. Chen, Y.; Li, G.; Yang, F.; Zhang, S. Mn/ZSM-5 participation in the degradation of cellulose under phosphoric acid media. *Polym. Degrad. Stab.* **2011**, *96*, 863–869. [CrossRef]
5. Abels, C.; Thimm, K.; Wulfhorst, H.; Christine, A.; Wessling, M. Bioresource Technology Membrane-based recovery of glucose from enzymatic hydrolysis of ionic liquid pretreated cellulose. *Bioresour. Technol.* **2013**, *149*, 58–64. [CrossRef]
6. Wang, J.; Xi, J.; Wang, Y. Recent advances in the catalytic production of glucose from lignocellulosic biomass. *Green Chem.* **2015**, *17*, 737–751. [CrossRef]
7. Verendel, J.; Church, T.; Andersson, P. Catalytic One-Pot Production of Small Organics from Polysaccharides. *Synthesis* **2011**, *2011*, 1649–1677. [CrossRef]
8. Vo, H.T.; Widyaya, V.T.; Jae, J.; Kim, H.S.; Lee, H. Hydrolysis of ionic cellulose to glucose. *Bioresour. Technol.* **2014**, *167*, 484–489. [CrossRef]
9. Huang, Y.-B.; Fu, Y. Hydrolysis of cellulose to glucose by solid acid catalysts. *Green Chem.* **2013**, *15*, 1095. [CrossRef]
10. Brandt, A.; Gräsvik, J.; Hallett, J.P.; Welton, T. Deconstruction of lignocellulosic biomass with ionic liquids. *Green Chem.* **2013**, *15*, 550–583. [CrossRef]
11. Fukaya, Y.; Hayashi, K.; Ohno, H. Cellulose dissolution with polar ionic liquids under mild conditions: Required factors for anions. *Green Chem.* **2008**, *1*, 44–46. [CrossRef]
12. Tong, X.; Ma, Y.; Li, Y. Applied Catalysis A: General Biomass into chemicals: Conversion of sugars to furan derivatives by catalytic processes. *Appl. Catal. A Gen.* **2010**, *385*, 1–13. [CrossRef]
13. Kassaye, S.; Pagar, C.; Pant, K.K.; Jain, S.; Gupta, R. Bioresource Technology Depolymerization of microcrystalline cellulose to value added chemicals using sulfate ion promoted zirconia catalyst. *Bioresour. Technol.* **2016**, *220*, 394–400. [CrossRef] [PubMed]
14. Cao, X.; Peng, X.; Sun, S.; Zhong, L.; Wang, S.; Lu, F.; Sun, R. Impact of regeneration process on the crystalline structure and enzymatic hydrolysis of cellulose obtained from ionic liquid. *Carbohydr. Polym.* **2014**, *111*, 400–403. [CrossRef] [PubMed]
15. Ding, Y.-L.; Wang, H.-Q.; Xiang, M.; Yu, P.; Li, R.-Q.; Ke, Q.-P. The Effect of Ni-ZSM-5 Catalysts on Catalytic Pyrolysis and Hydro-Pyrolysis of Biomass. *Front. Chem.* **2020**, *8*, 790. [CrossRef]
16. Zhao, C.; Kasakov, S.; He, J.; Lercher, J.A. Comparison of kinetics, activity and stability of Ni/HZSM-5 and Ni/Al2O3-HZSM-5 for phenol hydrodeoxygenation. *J. Catal.* **2012**, *296*, 12–23. [CrossRef]
17. Topsøe, N.-Y.; Pedersen, K.; Derouane, E.G. Infrared and temperature-programmed desorption study of the acidic properties of ZSM-5-type zeolites. *J. Catal.* **1981**, *70*, 41–52. [CrossRef]
18. Kosinov, N.; Liu, C.; Hensen, E.J.M.; Pidko, E.A. Engineering of Transition Metal Catalysts Confined in Zeolites. *Chem. Mater.* **2018**, *30*, 3177–3198. [CrossRef]
19. Rout, P.K.; Nannaware, A.D.; Prakash, O.; Kalra, A.; Rajasekharan, R. Synthesis of hydroxymethylfurfural from cellulose using green processes: A promising biochemical and biofuel feedstock. *Chem. Eng. Sci.* **2016**, *142*, 318–346. [CrossRef]
20. Kassaye, S.; Pant, K.K.; Jain, S. Synergistic effect of ionic liquid and dilute sulphuric acid in the hydrolysis of microcrystalline cellulose. *Fuel Process. Technol.* **2016**, *148*, 289–294. [CrossRef]
21. Van der Bij, H.E.; Weckhuysen, B.M. Local silico-aluminophosphate interfaces within phosphated H-ZSM-5 zeolites. *Phys. Chem. Chem. Phys.* **2014**, *16*, 29–32. [CrossRef] [PubMed]
22. He, D.; Wang, X.; Yang, Y.; He, R.; Zhong, H.; Wang, Y.; Jin, F. Hydrothermal synthesis of long-chain hydrocarbons up to C24 with $NaHCO_3$-assisted stabilizing cobalt. *Proc. Natl. Acad. Sci. USA* **2021**, *118*, e2115059118. [CrossRef] [PubMed]
23. Yumura, T.; Hasegawa, S.; Itadani, A.; Kobayashi, H.; Kuroda, Y. The Variety of Carbon-Metal Bonds inside Cu-ZSM-5 Zeolites: A Density Functional Theory Study. *Materials* **2010**, *3*, 2516. [CrossRef]
24. Atkins, P.W.; Atkins, P.W. *Shriver & Atkins Inorganic Chemistry*; Oxford University Press: Oxford, UK, 2006.
25. Yumura, T.; Takeuchi, M.; Kobayashi, H.; Kuroda, Y. Effects of ZSM-5 zeolite confinement on reaction intermediates during dioxygen activation by enclosed dicopper cations. *Inorg. Chem.* **2009**, *48*, 508–517. [CrossRef] [PubMed]
26. Kostyniuk, A.; Key, D.; Mdleleni, M. Effect of Fe-Mo promoters on HZSM-5 zeolite catalyst for 1-hexene aromatization. *J. Saudi Chem. Soc.* **2019**, *23*, 612–626. [CrossRef]
27. Xiao, P.; Wang, Y.; Kondo, J.N.; Yokoi, T. Consequences of Fe speciation in MFI zeolites for hydroxylation of benzene to phenol with H2O2. *Appl. Catal. A Gen.* **2019**, *579*, 159–167. [CrossRef]

28. Mimura, N.; Okamoto, M.; Yamashita, H.; Oyama, S.T.; Murata, K. Oxidative dehydrogenation of ethane over Cr/ZSM-5 catalysts using CO2 as an oxidant. *J. Phys. Chem. B* **2006**, *110*, 21764–21770. [CrossRef]
29. Cai, H.; Li, C.; Wang, A.; Xu, G.; Zhang, T. Applied Catalysis B: Environmental Zeolite-promoted hydrolysis of cellulose in ionic liquid, insight into the mutual behavior of zeolite, cellulose and ionic liquid. *Appl. Catal. B Environ.* **2012**, *123–124*, 333–338. [CrossRef]
30. Liu, H.; Wei, H.; Xin, W.; Song, C. Differences between Zn / HZSM-5 and Zn / HZSM-11 zeolite catalysts in alkylation of benzene with dimethyl ether. *J. Energy Chem.* **2014**, *23*, 617–624. [CrossRef]
31. Yang, H.; Fairbridge, C.; Ring, Z.; Hawkins, R.; Hill, J.M. Hydrogenation and mild hydrocracking of synthetic crude distillate by Pt-supported mesoporous material catalysts. In *Studies in Surface Science and Catalysis*; Sayari, A., Jaroniec, M., Eds.; Elsevier: Amsterdam, The Netherlands, 2002; Volume 141, pp. 543–552.
32. Farrauto, R.J.; Hobson, M.C. Catalyst Characterization. In *Encyclopedia of Physical Science and Technology*, 3rd ed.; Meyers, R.A., Ed.; Academic Press: New York, NY, USA, 2003; pp. 501–526.
33. Arango, A.M.S.; Garcés, C.M.E.; Valderrama, J.L.A.; Monsalve, A.G.; Santos, L.A.P.; Isaza, A.E. Oligomerization of propene over ZSM-5 modified with Cr and W. *Rev. Fac. Ing.* **2011**, *57*, 57–65.
34. Benaliouche, F.; Boucheffa, Y.; Ayrault, P.; Mignard, S.; Magnoux, P. NH3-TPD and FTIR spectroscopy of pyridine adsorption studies for characterization of Ag-and Cu-exchanged X zeolites. *Microporous Mesoporous Mater.* **2008**, *111*, 80–88. [CrossRef]
35. Hosseinpour, M.; Akizuki, M.; Yoko, A.; Oshima, Y.; Soltani, M. Novel synthesis and characterization of Fe-ZSM-5 nanocrystals in hot compressed water for selective catalytic reduction of NO with NH_3. *Microporous Mesoporous Mater.* **2020**, *292*, 109708. [CrossRef]
36. Baek, I.G.; You, S.J.; Park, E.D. Bioresource Technology Direct conversion of cellulose into polyols over Ni/W/SiO_2-Al_2O_3. *Bioresour. Technol.* **2012**, *114*, 684–690. [CrossRef] [PubMed]
37. Celik, F.E.; Kim, T.-J.; Bell, A.T. Effect of zeolite framework type and Si/Al ratio on dimethoxymethane carbonylation. *J. Catal.* **2010**, *270*, 185–195. [CrossRef]
38. Zhang, R.; Zhang, B.; Shi, Z.; Liu, N.; Chen, B. Catalytic behaviors of chloromethane combustion over the metal-modified ZSM-5 zeolites with diverse SiO2/Al2O3 ratios. *J. Mol. Catal. A Chem.* **2015**, *398*, 223–230. [CrossRef]
39. Bali, S.; Tofanelli, M.A.; Ernst, R.D.; Eyring, E.M. Chromium (III) catalysts in ionic liquids for the conversion of glucose to 5-(hydroxymethyl) furfural (HMF): Insight into metal catalyst: Ionic liquid mediated conversion of cellulosic biomass to biofuels and chemicals. *Biomass Bioenergy* **2012**, *42*, 224–227. [CrossRef]
40. Zhao, H.; Holladay, J.E.; Brown, H.; Zhang, Z.C. Metal Chlorides in Ionic Liquid Solvents Convert Sugars to 5-Hydroxymethylfurfural. *Science* **2007**, *316*, 1597–1600. [CrossRef]
41. Xu, H.; Miao, Z.; Zhao, H.; Yang, J.; Zhao, J.; Song, H.; Liang, N.; Chou, L. Dehydration of fructose into 5-hydroxymethylfurfural by high stable ordered mesoporous zirconium phosphate. *Fuel* **2015**, *145*, 234–240. [CrossRef]
42. Hu, L.; Wu, Z.; Xu, J.; Sun, Y.; Lin, L.; Liu, S. Zeolite-promoted transformation of glucose into 5-hydroxymethylfurfural in ionic liquid. *Chem. Eng. J.* **2014**, *244*, 137–144. [CrossRef]
43. Saeman, J.F. Hydrolysis of Cellulose and Decomposition of Sugars in Dilute Acid at High Temperature. *Ind. Eng. Chem.* **1945**, *37*, 43–52. [CrossRef]
44. Lai, Y.; Veser, G. The nature of the selective species in Fe-HZSM-5 for non-oxidative methane dehydroaromatization. *Catal. Sci. Technol.* **2016**, *6*, 5440–5452. [CrossRef]
45. Negahdar, L.; Delidovich, I.; Palkovits, R. Aqueous-phase hydrolysis of cellulose and hemicelluloses over molecular acidic catalysts: Insights into the kinetics and reaction mechanism. *Appl. Catal. B Environ.* **2016**, *184*, 285–298. [CrossRef]
46. Guo, F.; Fang, Z.; Xu, C.C.; Smith, R.L. Solid acid mediated hydrolysis of biomass for producing biofuels. *Prog. Energy Combust. Sci.* **2012**, *38*, 672–690. [CrossRef]
47. Hu, L.; Zhao, G.; Tang, X.; Wu, Z.; Xu, J.; Lin, L.; Liu, S. Catalytic conversion of carbohydrates into 5-hydroxymethylfurfural over cellulose-derived carbonaceous catalyst in ionic liquid. *Bioresour. Technol.* **2013**, *148*, 501–507. [CrossRef]